Frontier Orbitals of Trivalent Cages: (3,6) Cages and (4,6) Cages

S. Compernolle* and A. Ceulemans

Laboratorium voor Kwantumchemie, Katholieke Universiteit Leuven, Celestijnenlaan 200F, B-3001 Heverlee, Belgium

Received: November 25, 2004; In Final Form: January 17, 2005

A qualitative molecular-orbital treatment and group-theoretical analysis reveals the nature of the frontier orbitals of (3,6) and (4,6) polyhedral cages, consisting of a hexagonal network with triangular and square defects, respectively. Leapfrog (3,6) cages have two nonbonding filled orbitals. Leapfrog (4,6) cages have a high HOMO−LUMO gap, while nonleapfrog (4,6) cages with octahedral symmetry have a very small HOMO−LUMO gap. The symmetry of the frontier orbitals is determined.

1. Introduction

The discovery of fullerenes has revived the study of the mathematics of polyhedral cages. Physicists and chemists show a special interest in cages that can be folded from a honeycomb lattice by introducing pentagonal, triangular, or square defects. Combining Hückel theory with a group-theoretical analysis, Fowler and Ceulemans[1] proved that any fullerene of the leapfrog class has six low-lying empty molecular orbitals (MOs)—spanning the translational and rotational symmetries—above the highest occupied molecular orbital (HOMO). These MOs can therefore act as electron acceptor levels. In this paper, we extend this analysis to leapfrog cages consisting of hexagons and four triangles ((3,6) cages)[2] and leapfrog and nonleapfrog cages consisting of hexagons and six squares ((4,6) cages).[3] Several studies have been devoted to the boron nitride analogues of (4,6) cages,[4−12] and there is evidence for their experimental synthesis.[13,14] All possible symmetries have been found for (3,6) cages[15] and (4,6) cages.[16]

Leapfrog and nonleapfrog (3,6) cages, with symmetries ranging from D_2 to T_d, were investigated in ref 2. A zone-folding procedure allowed a complete breakdown of the Hückel eigenenergies, MOs, and their symmetries. Leapfrog and nonleapfrog (4,6) cages with octahedral symmetry were treated in ref 3. The Hückel energies, MOs, and their symmetries were obtained by a zone-folding procedure but only for the A_1, A_2, and E representations. Numerical calculations on a large set of cages revealed that the frontier orbitals were always of T_1 and T_2 symmetry and that the leapfrog (4,6) cages have a much larger gap between the HOMO and the lowest unoccupied molecular orbital (LUMO) than the nonleapfrog cages. The group-theoretical study in this paper explains the origin of this behavior, and is not restricted to cages with octahedral symmetry.

2. The Two Bonding Extremes: Fries and Clar

Three different types of polyhedra are studied in this work: leapfrog (3,6) cages, leapfrog (4,6) cages, and nonleapfrog (4,6) cages. (A leapfrog polyhedron C_n is constructed in imagination from a smaller parent polyhedron $C_{n/3}$ by first capping all faces and then taking the dual of the resulting polyhedron.[17]) For all three, it is possible to draw two extreme bonding schemes: a Fries limit and a Clar limit.[18] The definition given here is not restricted to leapfrog structures.[17] Consider first the following selection procedure.

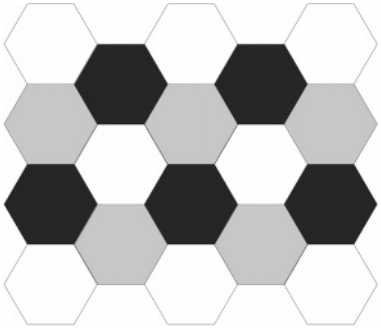

Figure 1. The three independent colorings (gray, white, and black) on the honeycomb lattice that obey criterion 1.

Select one face and color it. Color also all other faces that are connected to this first face by following the bonds that are radiating from the first face. Repeat this procedure for all colored faces until no new faces can be colored anymore. The colored faces must now obey the following criterion:

Criterion 1. *The colored faces exhaust all the vertexes. None of the colored faces may share sides, but all are connected by bonds.*

This coloring procedure can also be applied to the honeycomb lattice. Three independent colorings are possible based on criterion 1. Figure 1 shows that the faces of the honeycomb lattice are distributed among three equivalent disjoint sets: gray, white, and black faces.

The polyhedra can be thought of as being derived from the honeycomb lattice, by cutting out wedges with starting points in the middle of a hexagonal face of the honeycomb lattice. Figure 2a (b) shows how a wedge with an angle of $^{\pi}/_{3}$ (π) is cut out from the honeycomb lattice to introduce a pentagonal (trigonal) defect. Suppose the first wedge has its starting point in the middle of a gray face. The set of gray faces is still consistent with criterion 1, but the white and black faces no longer are. Thus, cutting out one sector already reduces the number of independent colorings from three to one. Introducing new defects, their corresponding wedges should also have their starting point on gray faces; otherwise, also the set of gray faces is no longer in agreement with criterion 1.

10.1021/jp0446229 CCC: $30.25
Published on Web 02/23/2005

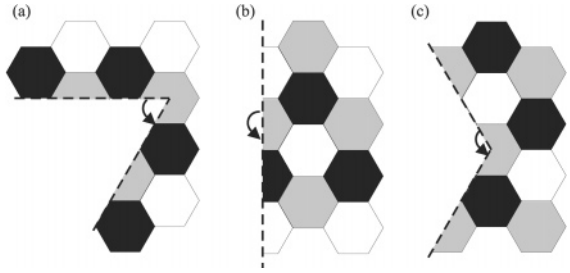

Figure 2. Cutting out wedges from the honeycomb lattice to introduce nonhexagonal faces, for pentagonal (a), trigonal (b), and tetragonal (c) defects.

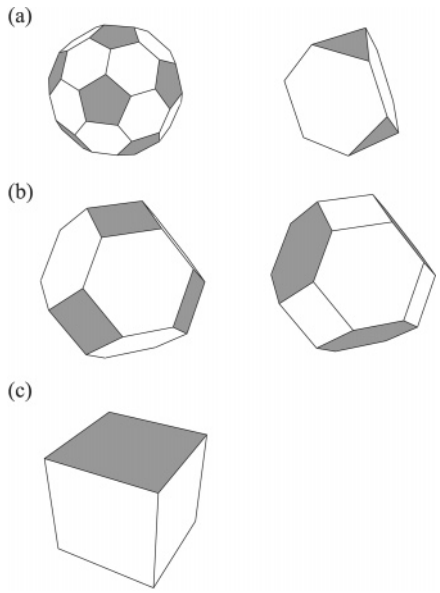

Figure 3. Coloring of some of the faces of polyhedra such that criterion 1 is obeyed. (a) The simplest leapfrog fullerene and leapfrog (3,6) cage. There is only one possibility: the colored faces correspond to that of the parent cage. (b) The simplest leapfrog (4,6) cage. Three different colorings are possible, of which only two are shown (the third one is equivalent to the second). (c) The simplest nonleapfrog (4,6) cage: the cube. Three different colorings are possible, of which only one is shown (the other two are equivalent to this one).

However, the case is different when introducing tetragonal defects in the honeycomb lattice. Cutting out a sector with an angle of $^{2\pi}/_{3}$ never creates an inconsistency with criterion 1 for gray, white, or black faces (Figure 2c). Thus, introducing tetragonal defects does not affect the three independent colorings.

In summary, the following cases are possible for (3,6) and (4,6) cages and fullerenes:

(1) (3,6) cages and fullerenes where no coloring based on criterion 1 is possible. These cages are nonleapfrogs and will not be treated in this work.

(2) (3,6) cages and fullerenes where one of the three colorings still obeys criterion 1 (Figure 3a). These cages are leapfrogs. The colored faces of the leapfrog structure **L** are derived from the faces of the parent structure **P** (and hence the nonhexagonal faces will always be among them), and the bonds that connect them are derived from the bonds of the parent structure. Since **P** has the same symmetry as **L**, the coloring does not reduce the symmetry of **L**.

(3) (4,6) cages, both leapfrog and nonleapfrog, always have three independent colorings that obey criterion 1. Let us call the uncolored structure **S** with point group G and group order g and the three colored structures $\mathbf{S}_1$, $\mathbf{S}_2$, and $\mathbf{S}_3$ with groups G_1, G_2, and G_3 and group orders g_1, g_2, and g_3, respectively. G_1, G_2, and G_3 are always subgroups of G. Three possibilities for the point groups of the colored (4,6) cages exist in principle. (i) None of the symmetry elements of **S** interchange any of the three colored cages $\mathbf{S}_1$, $\mathbf{S}_2$, and $\mathbf{S}_3$. We then have $G = G_1 = G_2 = G_3$. (ii) One of the colored cages (say $\mathbf{S}_1$) is unchanged by any of the symmetry elements of **S**, while some symmetry elements interchange $\mathbf{S}_2$ and $\mathbf{S}_3$. We then have $G = G_1$, while $G_2 = G_3$ and $g_2 = g_3 = g/2$. (iii) **S** has one or more C_3 axes that convert $\mathbf{S}_1$ to $\mathbf{S}_2$, $\mathbf{S}_2$ to $\mathbf{S}_3$, and $\mathbf{S}_3$ to $\mathbf{S}_1$. G_1, G_2, and G_3 are then isomorphic subgroups of G, and $g_1 = g_2 = g_3 = g/3$.

For a leapfrog (4,6) cage $\mathbf{S} = \mathbf{L}$, the colored faces of one of the three colored structures (say $\mathbf{S}_1$) correspond to the faces of the parent structure **P** (and hence the squares will always be among them) and the interconnecting bonds to the bonds of **P** (Figure 3b). The coloring does not reduce the symmetry of **L** in this case. $\mathbf{S}_2$ and $\mathbf{S}_3$ have no squares among their colored faces. Only cases i and ii are possible here.

None of the three colored structures of a nonleapfrog (4,6) cage contain all of the six squares (Figure 3c). Cases i−iii are possible here.

Suppose a coloring is possible for the structure **S**, which has n atoms. **S** is trivalent, so the number of edges is $e = 3n/2$. The edges that connect the colored faces exhaust all vertexes but are not connected to each other, so their number is $n/2$.

We work within the simple Hückel approximation: the interaction between all nearest neighbors is described by the same parameter β ($\beta < 0$), and the energy of all the atoms, by the same parameter α. The Hückel Hamiltonian $\mathbf{H}(\mathbf{S})$ is then equal to

$$\mathbf{H}(\mathbf{S}) = \alpha\mathbf{I} + \beta\mathbf{A}(\mathbf{S}) \tag{1}$$

where $\mathbf{A}(\mathbf{S})$ is the connectivity matrix of structure **S**.

The Fries limit of **S**, $\mathbf{F_S}$, is obtained by attributing formal double bonds to the $n/2$ edges that connect the colored faces and single bonds to all other edges. β is set to zero for all single bonds. One has now $n/2$ isolated bonds and hence $n/2$ bonding orbitals (labeled π) at energy $E = \alpha + \beta$ and $n/2$ antibonding orbitals (labeled π^*) at energy $E = \alpha - \beta$. Since there are n electrons in the neutral structure, the Fries limit constitutes a closed shell π electronic configuration.

The Clar limit of **S**, $\mathbf{C_S}$, is obtained by setting β to zero for all bonds that connect the colored faces. One obtains now a system of isolated polygons, and the orbitals of these polygons can be labeled as σ, π, δ, ... We will denote the orbital σ of a j-gon by σ_j, and similarly for the other orbitals.

The two limits are each other's complement, in the sense that the sum of the connectivity matrix of the Fries structure $\mathbf{F_S}$ and that of the Clar structure $\mathbf{C_S}$ gives the connectivity matrix of the total structure **S**:

$$\mathbf{A}(\mathbf{F_S}) + \mathbf{A}(\mathbf{C_S}) = \mathbf{A}(\mathbf{S}) \tag{2}$$

These two bonding extremes can be connected in a Walsh-like correlation diagram, which gives information about the frontier orbitals of these structures. At any point between these two extremes, the Hamiltonian is given by

$$\mathbf{H}' = \alpha\mathbf{I} + \beta_F\mathbf{A}(\mathbf{F_S}) + \beta_C\mathbf{A}(\mathbf{C_S}) \tag{3}$$

The Fries limit is obtained by setting $\beta_F = \beta$ and $\beta_C = 0$, and the Clar limit, by setting $\beta_F = 0$ and $\beta_C = \beta$. The actual structure is formally identified to the center of the correlation diagram where $\beta_F = \beta_C = \beta$.

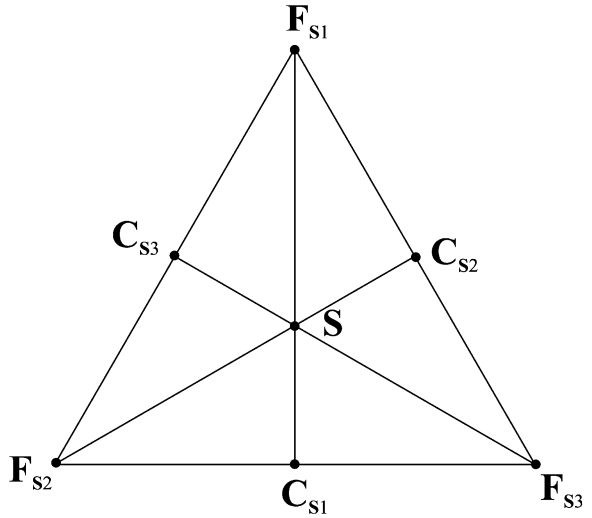

Figure 4. Fries (**F**) and Clar (**C**) reference points for the two-dimensional Walsh diagram of (4,6) cages.

When three different Fries/Clar structures are possible, the connectivity matrix is equal to

$$\mathbf{A}(\mathbf{S}) = \mathbf{A}(\mathbf{F}_{S_1}) + \mathbf{A}(\mathbf{F}_{S_2}) + \mathbf{A}(\mathbf{F}_{S_3}) = \frac{1}{2}(\mathbf{A}(\mathbf{C}_{S_1}) + \mathbf{A}(\mathbf{C}_{S_2}) + \mathbf{A}(\mathbf{C}_{S_3})) \quad (4)$$

One has now three independent extremes, $\mathbf{F}_{S_1}$, $\mathbf{F}_{S_2}$, and $\mathbf{F}_{S_3}$. The three Clar extremes are linearly dependent on these, since $\mathbf{A}(\mathbf{C}_{S_1}) = \mathbf{A}(\mathbf{F}_{S_2}) + \mathbf{A}(\mathbf{F}_{S_3})$ and similarly for the other Clar extremes. At any point between these three extremes, the Hamiltonian is given by

$$\mathbf{H}'' = \alpha\mathbf{I} + \beta_{F_1}\mathbf{A}(\mathbf{F}_{S_1}) + \beta_{F_2}\mathbf{A}(\mathbf{F}_{S_2}) + \beta_{F_3}\mathbf{A}(\mathbf{F}_{S_3}) \quad (5)$$

The Walsh diagram is now two-dimensional, as shown in Figure 4.

To simplify further discussion, we set $\alpha = 0$. Also, in this case, the center of the diagram is identified as the reference structure of the Hückel treatment.

3. Preliminary Group-Theoretical Lemmas

3.1. Leapfrog Cages. In this section, we recall a general result[1] about orbital symmetry representations in leapfrog cages.

In the Fries limit, the localized bonding orbitals of the leapfrog cage $\mathbf{S} = \mathbf{L}$ with n atoms span the permutation representation of the $n/2$ edges of the parent **P**:

$$\Gamma(\mathbf{F}_\mathbf{L}, E < 0) = \Gamma_\sigma(e, \mathbf{P}) \quad (6)$$

where Γ denotes a (reducible) symmetry representation and σ indicates that edge bonds are totally symmetric with respect to all symmetry elements that go through the edge.

The number of isolated faces of the leapfrog cage is equal to the number of faces of the parent cage, and following Euler's theorem, this is equal to $n/6 + 2$. Consider the σ, π_x, and π_y orbitals of the isolated polygons of $\mathbf{C}_\mathbf{L}$, $3(n/6 + 2) = n/2 + 6$ orbitals in total. Their symmetry is obtained by multiplying the permutation representation of the parent faces by the translational symmetry, that is, from the product $\Gamma_\sigma(f, \mathbf{P}) \times \Gamma_\mathrm{T}$:

$$\Gamma(\mathbf{C}_\mathbf{L}, \sigma + \pi) = \Gamma_\sigma(f, \mathbf{P}) \times \Gamma_\mathrm{T} \quad (7)$$

This product is simply the sum of the permutation representation of its edges and the translational and rotational symmetries:[19]

$$\Gamma_\sigma(f, \mathbf{P}) \times \Gamma_\mathrm{T} = \Gamma_\sigma(e, \mathbf{P}) + \Gamma_\mathrm{T} + \Gamma_\mathrm{R} \quad (8)$$

and therefore

$$\Gamma(\mathbf{C}_\mathbf{L}, \sigma + \pi) = \Gamma(\mathbf{F}_\mathbf{L}, E < 0) + \Gamma_\mathrm{T} + \Gamma_\mathrm{R} \quad (9)$$

These equations will prove essential to get insight into the arrangement of the frontier orbitals of leapfrog cages.

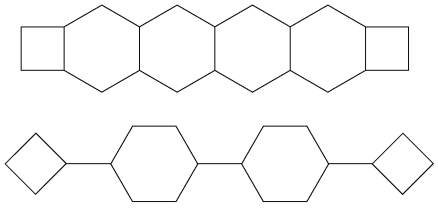

Figure 5. Two squares in a zigzag relation (top) and an armchair relation (bottom).

3.2. (4,6) Cages: Alternants. A (4,6) cage is an alternant: its vertexes can be divided into two equal sets, black and white, such that every vertex of one set is surrounded by members of the other. As a consequence, its spectrum is bipartite: for each bonding MO at energy $E < 0$, there exists an antibonding MO at energy $-E > 0$ with the same coefficient on white vertexes but an opposite value on black vertexes;[20,21] the spectrum has mirror symmetry around the nonbonding level. Since the number of black and white vertexes is equal, eventual nonbonding MOs also occur in such pairs.

Any symmetry operation will *either* map black vertexes on black vertexes and white vertexes on white vertexes *or* exchange black and white vertexes. The proof goes as follows: Suppose a symmetry operation $\mathscr{R}$ would map the black vertex $v_1^\bullet$ on the black vertex $v_2^\bullet$ and the white vertex v_3° on the black vertex $v_4^\bullet$. $v_1^\bullet$ and v_3° are connected by a path of edges. When $v_1^\bullet$ and v_3° are taken into account, there is an even number of vertexes, alternating black and white, along this path. Acting with $\mathscr{R}$ on this path, one obtains a path connecting $v_2^\bullet$ and $v_4^\bullet$. However, this path also contains an even number of vertexes; hence, it is impossible that the first and last vertexes are both black. Thus, we have proven that any symmetry operator will map vertexes on vertexes of the same color ($\mathscr{R}_{\bullet\to\bullet}$) or will map vertexes on vertexes of different colors ($\mathscr{R}_{\bullet\to\circ}$). Let us define now the following one-dimensional representation Γ_{-1}.

$$\chi^{\Gamma_{-1}}(\mathscr{R}_{\bullet\to\bullet}) = 1$$
$$\chi^{\Gamma_{-1}}(\mathscr{R}_{\bullet\to\circ}) = -1 \quad (10)$$

Γ_{-1} is necessarily an irreducible representation, since it is the representation of the totally antibonding MO. Γ_{-1} relates the symmetries of every pair of MOs at opposite energies:

$$\Gamma_{-1} \times \Gamma(E) = \Gamma(-E) \quad (11)$$

Γ_{-1} is equal to A_2 for cages with O symmetry, to A_{2g} for cages with O_h symmetry and with neighboring defects in an armchair relation, and to A_{2u} for cages with O_h symmetry and with the neighboring defects in a zigzag relation (see Figure 5).

(4,6) cages can also be inscribed on hexagonal prisms,[5] with a resulting symmetry of D_6 ($\Gamma_{-1} = B_2$) or D_{6h} ($\Gamma_{-1} = B_{2g}$). Γ_{-1} can be derived from these cases when the cage has a lower symmetry.

4. Leapfrog Fullerenes

The application of the Walsh-type analysis to the case of leapfrog fullerenes has been presented in ref 1. Here, we briefly recall the results.

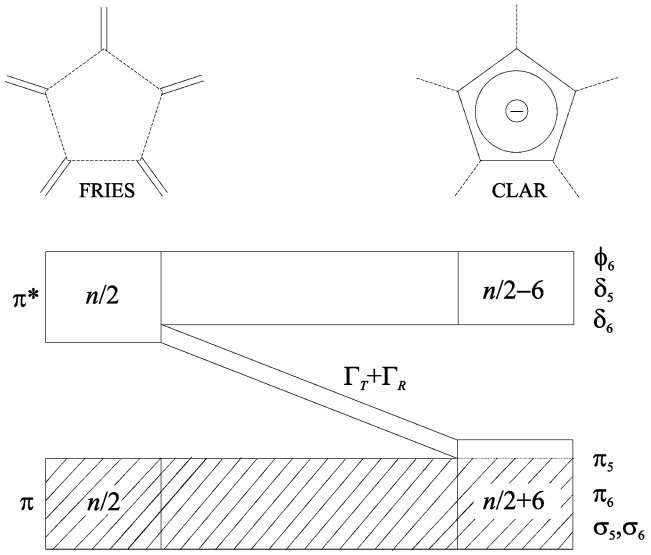

Figure 6. Walsh diagram for leapfrog fullerenes with correlation between two bonding extremes: the Fries limit (left) and the Clar limit (right). The hatched region denotes occupied orbitals in the neutral cage.

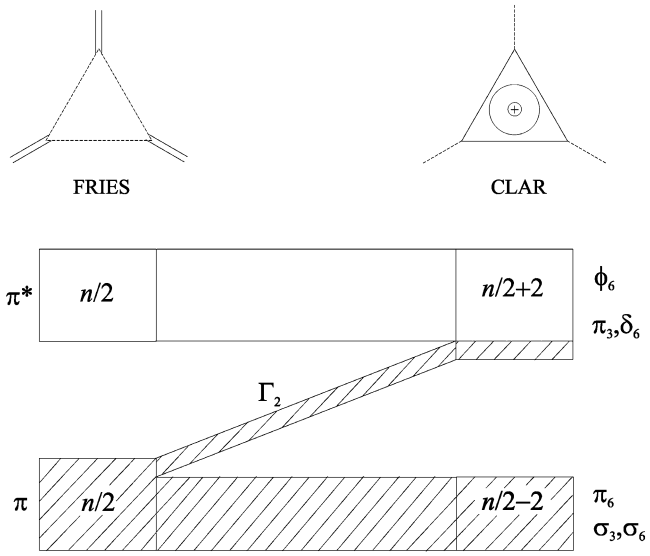

Figure 7. Walsh diagram for leapfrog (3,6) cages with correlation between two bonding extremes: the Fries limit (left) and the Clar limit (right).

In the Clar limit, the σ and π orbitals of the isolated hexagons and pentagons are all bonding, while the other orbitals are antibonding

$$\Gamma(\mathbf{C_L}, \sigma + \pi) = \Gamma(\mathbf{C_L}, E < 0) \tag{12}$$

Taking the difference of the symmetries of the orbitals bonding in the Clar limit with those bonding in the Fries limit, one obtains from eq 9

$$\Gamma(\mathbf{C_L}, E < 0) - \Gamma(\mathbf{F_L}, E < 0) = \Gamma_T + \Gamma_R \tag{13}$$

Figure 6 shows the general Walsh diagram. Because of the noncrossing rule,[22] all bonding orbitals in the Fries limit are matched by bonding orbitals in the Clar limit. Six orbitals, spanning the symmetry $\Gamma_T + \Gamma_R$, are bonding in the Clar limit and antibonding in the Fries limit, and hence, they will be close to nonbonding in the neutral fullerene, lying above the $n/2$ occupied bonding orbitals. They thus constitute the six lowest unoccupied MOs of the cage, and this explains the electron-accepting behavior of the leapfrog fullerenes. However, the six orbitals will still be slightly antibonding; a theorem proven by Manolopoulos et al.[23] states that any leapfrog polyhedron with at least one face not divisible by 3 will have a closed shell with a strictly bonding HOMO and a strictly antibonding LUMO.

5. Leapfrog (3,6) Cages

Consider the σ and π orbitals of the isolated hexagons and triangles of the Clar limit. The eight π_3 orbitals are antibonding, while the other orbitals are bonding. The symmetry of these antibonding orbitals is given by

$$\Gamma(\mathbf{C_L}, \pi_3) = \Gamma_\sigma(f_3, \mathbf{P}) \times \Gamma_T - \Gamma_\sigma(f_3, \mathbf{P}) \tag{14}$$

with $\Gamma(\mathbf{C_L}, \pi_3)$ spanning the symmetries of the π orbitals on the triangles and $\Gamma_\sigma(f_3, \mathbf{P}) = \Gamma(\mathbf{C_L}, \sigma_3)$ spanning those of the σ orbitals. Suppose the structure **L** has the highest possible symmetry, T_d. The symmetry of the eight trigonal π orbitals is then

$$\Gamma(\mathbf{C_L}, \pi_3) = T_1 + T_2 + E \tag{15}$$

so the translational and rotational symmetries ($\Gamma_T = T_2$ and $\Gamma_R = T_1$) are contained in $\Gamma(\mathbf{C_L}, \pi_3)$, and this stays true for lower symmetries. For arbitrary symmetry, one can say

$$\Gamma(\mathbf{C_L}, \pi_3) = \Gamma_T + \Gamma_R + \Gamma_2 \tag{16}$$

where Γ_2 is a two-dimensional term. The symmetry of the bonding orbitals in the Clar limit is spanned by

$$\begin{aligned}\Gamma(\mathbf{C_L}, E < 0) &= \Gamma(\mathbf{C_L}, \sigma_6 + \pi_6 + \sigma_3) \\ &= \Gamma_\sigma(f_6, \mathbf{P}) \times \Gamma_T + \Gamma_\sigma(f_3, \mathbf{P})\end{aligned} \tag{17}$$

with $\Gamma_\sigma(f_6, \mathbf{P}) = \Gamma(\mathbf{C_L}, \sigma_6)$ spanning the symmetries of the hexagonal faces of the parent structure. Combining this with eqs 7 and 14, one finds for the bonding orbitals in the Clar limit

$$\Gamma(\mathbf{C_L}, E < 0) = \Gamma_\sigma(f, \mathbf{P}) \times \Gamma_T - \Gamma(\mathbf{C_L}, \pi_3) \tag{18}$$

The bonding orbitals in the Fries limit are obtained by combining eqs 6 and 8 as

$$\Gamma(\mathbf{F_L}, E < 0) = \Gamma_\sigma(e, \mathbf{P}) = \Gamma_\sigma(f, \mathbf{P}) \times \Gamma_T - \Gamma_T - \Gamma_R \tag{19}$$

so the difference between the two is

$$\Gamma(\mathbf{F_L}, E < 0) - \Gamma(\mathbf{C_L}, E < 0) = \Gamma(\mathbf{C_L}, \pi_3) - \Gamma_T - \Gamma_R = \Gamma_2 \tag{20}$$

Figure 7 shows the general Walsh diagram. Two orbitals are bonding in the Fries limit, and hence occupied in the neutral cage, and antibonding in the Clar limit. This means that the two highest occupied orbitals of the (3,6) cage are close to nonbonding. In fact, they will be *exactly* nonbonding. A theorem proven by Fowler and Rogers[24] states that the two highest occupied MOs of any trivalent leapfrog polyhedron with all face sizes divisible by 3 and at least one face size not divisible by 6 will be exactly nonbonding. An illustrative example is given in Figure 8, showing the Walsh diagram for the simplest leapfrog (3,6) cage, C_{12}, with symmetry T_d. Two orbitals, spanning the symmetry $\Gamma_2 = E$, are indeed bonding in the Fries limit and antibonding in the Clar limit. At $\beta_C = \beta_F = \beta$, these doubly occupied orbitals are exactly nonbonding, and hence, they will act as electron-donating levels.

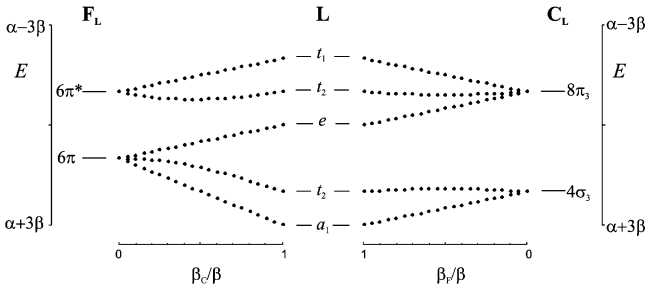

Figure 8. Correlation diagram for the orbital energies of the (3,6) cage C_{12}. From the left to the middle, β_C is increased from zero to β, while β_F is kept constant at β. From the middle to the right, β_F is diminished from β to zero, while β_C is kept constant at β. Degeneracies are not shown explicitly but can be deduced from the tetrahedral symmetry labels. The HOMO occurs at the top of the π band on the left and on the bottom of the π band on the right.

The conclusions are in agreement with the zone-folding treatment in ref 2: leapfrog (3,6) cages, with a symmetry ranging from D_2 to T_d, always have a closed shell with two filled exactly nonbonding orbitals. Hence, leapfrog (3,6) cages will act as electron donors, as opposed to leapfrog fullerenes.

6. Leapfrog (4,6) Cages

As mentioned before, it is possible to write three different Fries and Clar structures for (4,6) cages. In the case of leapfrog cages, one Fries/Clar couple is derived from the parent structure **P** and has the same symmetry as **L** and **P**. Let us call them $\mathbf{F_L}$ and $\mathbf{C_L}$. The point group of the other two Fries/Clar couples can be equal to that of **L** or can be a subgroup with a group order one-half of that of **L**. Let us consider a few examples of high symmetry. The symmetry of the three Fries/Clar couples is equal to O, T, and T for cages with O symmetry, to O, T_h, and T_h for cages with O_h symmetry and with neighboring defects in a zigzag relation (Figure 5, top), and to O, T_d, and T_d for cages with O_h symmetry and with the neighboring defects in an armchair relation (Figure 5, bottom).

The leapfrog (4,6) cages have a clear bond alternation. Calculating the π bond order for the leapfrog (4,6) cage C_{24}, one finds a value of 0.687 for the bonds between two squares and a value of only 0.404 for the bonds that are part of the squares. Thus, $\mathbf{F_L}$ is the more dominant pattern compared to the other two Fries structures, as already noted for the BN analogue $B_{12}N_{12}$.[10] Therefore, it seems reasonable to consider only the extremes $\mathbf{F_L}$ and $\mathbf{C_L}$ (i.e., only one line going through **S** in Figure 4), reducing effectively the problem to a one-dimensional correlation diagram.

Consider the σ and π orbitals of the isolated hexagons and squares of $\mathbf{C_L}$. The 12 π_4 orbitals are nonbonding, while the other orbitals are bonding. Applying eq 9, the symmetries of the bonding and nonbonding orbitals in the Clar limit are given by

$$\begin{aligned}\Gamma(\mathbf{C_L}, \sigma+\pi) &= \Gamma(\mathbf{C_L}, E \le 0)\\ &= \Gamma(\mathbf{F_L}, E < 0) + \Gamma_T + \Gamma_R \end{aligned} \tag{21}$$

Using eq 11, one finds that

$$\begin{aligned}\Gamma(\mathbf{C_L}, E \ge 0) &= \Gamma_{-1} \times \Gamma(\mathbf{F_L}, E < 0) + \Gamma_{-1} \times (\Gamma_T + \Gamma_R)\\ &= \Gamma(\mathbf{F_L}, E > 0) + \Gamma_{-1} \times (\Gamma_T + \Gamma_R)\end{aligned} \tag{22}$$

The symmetry spanned by the total set of MOs of the system is of course given by

$$\begin{aligned}\Gamma_{tot} &= \Gamma(\mathbf{C_L}, E < 0) + \Gamma(\mathbf{C_L}, E = 0) + \Gamma(\mathbf{C_L}, E > 0)\\ &= \Gamma(\mathbf{F_L}, E < 0) + \Gamma(\mathbf{F_L}, E > 0)\end{aligned} \tag{23}$$

From eqs 21 and 22, it follows that

$$\begin{aligned}\Gamma_{tot} &= \Gamma(\mathbf{C_L}, E \le 0) + \Gamma(\mathbf{C_L}, E \ge 0) - \Gamma(\mathbf{C_L}, E = 0)\\ &= \Gamma(\mathbf{F_L}, E < 0) + \Gamma_T + \Gamma_R + \Gamma(\mathbf{F_L}, E > 0) + \Gamma_{-1} \times (\Gamma_T + \Gamma_R) - \Gamma(\mathbf{C_L}, E = 0)\\ &= \Gamma_{tot} + \Gamma_T + \Gamma_R + \Gamma_{-1} \times (\Gamma_T + \Gamma_R) - \Gamma(\mathbf{C_L}, E = 0)\end{aligned} \tag{24}$$

Hence, the symmetry of the nonbonding orbitals in the Clar limit is spanned by

$$\Gamma(\mathbf{C_L}, \pi_4) = \Gamma(\mathbf{C_L}, E = 0) = \Gamma_T + \Gamma_R + \Gamma_{-1} \times (\Gamma_T + \Gamma_R) \tag{25}$$

Suppose the structure **L** has the highest possible symmetry, O_h. The symmetry of the 12 π_4 orbitals is then equal to

$$\begin{aligned}\Gamma(\mathbf{C_L}, \pi_4) &= T_{1u} + T_{1g} + T_{2u} + T_{2g}\\ &= T_{1u} + T_{1g} + A_{2g} \times (T_{1u} + T_{1g})\\ &= T_{1u} + T_{1g} + A_{2u} \times (T_{1u} + T_{1g})\end{aligned} \tag{26}$$

which is indeed in agreement with eq 25, both for zigzaglike and armchairlike arranged defects. Combining eqs 21, 22, and 25, one finds that

$$\begin{aligned}\Gamma(\mathbf{F_L}, E < 0) - \Gamma(\mathbf{C_L}, E < 0) &= \Gamma_{-1} \times (\Gamma_T + \Gamma_R)\\ \Gamma(\mathbf{F_L}, E > 0) - \Gamma(\mathbf{C_L}, E > 0) &= \Gamma_T + \Gamma_R\end{aligned} \tag{27}$$

All bonding orbitals in the Clar limit are matched by bonding orbitals in the Fries limit. This leaves six bonding orbitals in the Fries limit with the symmetry $\Gamma_{-1} \times (\Gamma_T + \Gamma_R)$, which are matched by one-half of the 12 nonbonding π_4 orbitals in the Clar limit. The other six nonbonding orbitals, spanning the symmetry $\Gamma_T + \Gamma_R$, are matched by antibonding orbitals in the Fries limit. The general Walsh diagram is shown in Figure 9a. Hence, the symmetry of the highest six occupied orbitals is given by $\Gamma_{-1} \times (\Gamma_T + \Gamma_R)$ and that of the lowest six unoccupied orbitals by $\Gamma_T + \Gamma_R$. No crossing from bonding to antibonding or vice versa occurs when moving from the Fries limit to the Clar limit, so the HOMO−LUMO gap is expected to be rather large. An example is given for the simplest leapfrog (4,6) cage, C_{24}, which has O_h symmetry, in Figure 10. The symmetry of the HOMO and HOMO−1 is indeed spanned by $\Gamma_{-1} \times (\Gamma_T + \Gamma_R) = T_{2u} + T_{2g}$, and these orbitals are nonbonding in $\mathbf{C_L}$ and bonding in $\mathbf{F_L}$. The symmetry of the LUMO and LUMO+1 is spanned by $\Gamma_T + \Gamma_R = T_{1u} + T_{1g}$, and these orbitals are nonbonding in $\mathbf{C_L}$ and antibonding in $\mathbf{F_L}$.

Numerical calculations were performed on a large set of octahedral (4,6) cages.[3] It was found that, for leapfrog cages with O (O_h) symmetry, the symmetry of the first six unoccupied MOs is spanned by $2T_1$ ($T_{1u} + T_{1g}$), while the symmetry of the highest six occupied MOs is spanned by $2T_2$ ($T_{2u} + T_{2g}$), in full agreement with our symmetry analysis.

It is not difficult to perform the analysis for the full two-dimensional correlation diagram. Figure 11 shows the evolution of the energy levels along the circumference of the master triangle in Figure 4.

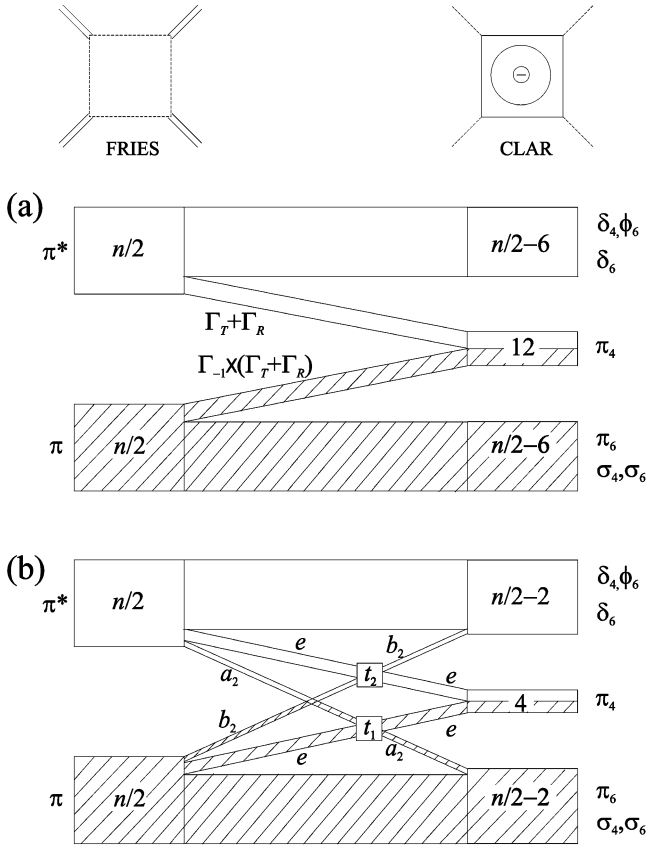

Figure 9. Walsh diagram for leapfrog (a) and octahedral nonleapfrog (b) (4,6) cages with correlation between two bonding extremes: the Fries limit (left) and the Clar limit (right).

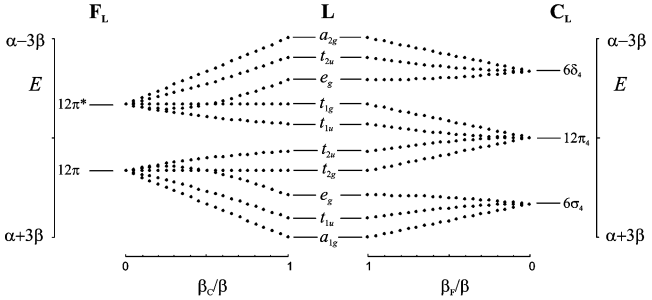

Figure 10. Correlation diagram for octahedral C_{24}. The conventions are similar to those of Figure 8. HOMO and HOMO−1 are bonding, and LUMO and LUMO+1 are antibonding in the Fries limit. All these orbitals are nonbonding in the Clar limit.

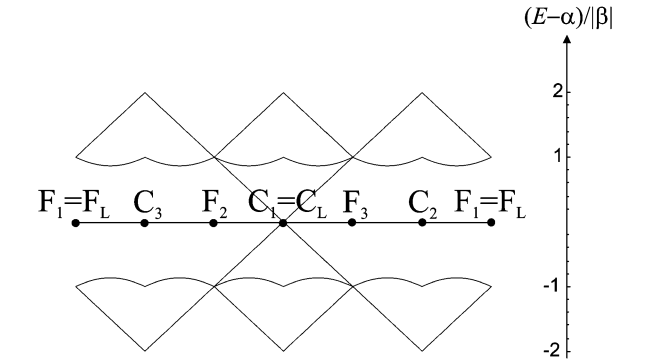

Figure 11. Correlation diagram for the MOs of a leapfrog (4,6) cage, following the circumference of the master triangle in Figure 4.

This diagram is actually nothing more than a superposition of correlations between different Kékulé structures of isolated hexagons and squares. When going around the circumference of the master triangle once, each energy level must of course end up at its starting point. This implies that it must cross the nonbonding energy an even number of times. However, Figure 11 makes it clear that there is only one point where energy levels become nonbonding, namely, at $\mathbf{C_L}$. Thus, all energy levels are either bonding on the border of the master triangle or antibonding, and at only one point, 12 levels will become nonbonding. This only strengthens the argument given above that leapfrog (4,6) cages will have a rather large HOMO−LUMO gap.

7. Nonleapfrog Octahedral (4,6) Cages

Also, nonleapfrog (4,6) cages have three different Fries structures and Clar counterparts. Only cages with *O* symmetry are considered in this section. For these cages, the number of atoms, *n*, is always a multiple of 8. The three Fries structures are then equivalent and similarly for the three Clar structures. The Clar limit has only orbitals on two of the six squares. The symmetry of an *O* (O_h) symmetrical cage **S** is reduced to D_4 (D_{4h}) when going to the Fries or the Clar extreme. At any other point in the triangle in Figure 4, the symmetry will be D_2 (D_{2h}). We choose now one Fries/Clar couple (which one is irrelevant) and consider the correlation between them (i.e., only one line in Figure 4 going through the center of the triangle).

Let us neglect mirror symmetry for simplicity. The four C_2 axes perpendicular to the principal C_4 axis go through hexagons when $n/8 = 2q$ (where q is an integer) and through edges when $n/8 = 2q + 1$. For symmetry reasons, these hexagons on the four C_2 axes must be part of the Clar pattern and the edges of the Fries pattern. Hence, the representations for the bonding orbitals in the Fries limit are given by

$$\Gamma(\mathbf{F_S}, E < 0) = \frac{n}{16} \times (A_1 + A_2 + B_1 + B_2 + 2E), \quad \text{for } \frac{n}{8} = 2q$$

$$\Gamma(\mathbf{F_S}, E < 0) = \frac{1}{2}\left(\frac{n}{8} - 1\right) \times (A_1 + A_2 + B_1 + B_2 + 2E) + A_1 + B_2 + E, \text{ for } \frac{n}{8} = 2q + 1 \quad (28)$$

The representations of the σ orbitals in the Clar limit are given by

$$\Gamma(\mathbf{C_S}, \sigma_4) = A_1 + A_2$$

$$\Gamma(\mathbf{C_S}, \sigma_6) = \frac{1}{6}\left(\frac{n}{8} - 4\right) \times (A_1 + A_2 + B_1 + B_2 + 2E) + A_1 + B_2 + E, \text{ for } \frac{n}{8} = 2q$$

$$\Gamma(\mathbf{C_S}, \sigma_6) = \frac{1}{6}\left(\frac{n}{8} - 1\right) \times (A_1 + A_2 + B_1 + B_2 + 2E), \quad \text{for } \frac{n}{8} = 2q + 1 \quad (29)$$

The π orbitals on the Clar faces are now easily obtained.

$$\begin{aligned}\Gamma(\mathbf{C_S}, \pi_4) &= \Gamma(\mathbf{C_S}, \sigma_4) \times \Gamma_T - \Gamma(\mathbf{C_S}, \sigma_4) \\ &= \Gamma(\mathbf{C_S}, \sigma_4) \times (A_2 + E) - \Gamma(\mathbf{C_S}, \sigma_4) \\ &= 2E = \Gamma(\mathbf{C_S}, E = 0)\end{aligned}$$

$$\Gamma(\mathbf{C_S}, \pi_6) = \Gamma(\mathbf{C_S}, \sigma_6) \times (A_2 + E) - \Gamma(\mathbf{C_S}, \sigma_6) = \frac{1}{3}\left(\frac{n}{8} - 1\right) \times (A_1 + A_2 + B_1 + B_2 + 2E) \quad (30)$$

The last equation holds both for $n/8$ even and odd. Combining eqs 28, 29, 30, and 11, one finds that

$$\Gamma(\mathbf{F_S}, E < 0) - \Gamma(\mathbf{C_S}, E < 0) = B_2 - A_2 + E$$
$$\Gamma(\mathbf{F_S}, E > 0) - \Gamma(\mathbf{C_S}, E > 0) = A_2 - B_2 + E \qquad (31)$$

Thus, one MO with B_2 symmetry is bonding in Fries and antibonding in Clar, and vice versa for a MO with A_2 symmetry. From the two MOs with E symmetry that are nonbonding in Clar, one will be bonding in Fries and the other antibonding in Fries. What does this mean for the structure **S** with O symmetry? Upon lowering the symmetry from O to D_4, the only way to obtain A_2, B_2, or E representations is

$$O \rightarrow D_4$$
$$T_1 \rightarrow A_2 + E$$
$$T_2 \rightarrow B_2 + E \qquad (32)$$

This already indicates that the symmetry of the three highest occupied orbitals and the three lowest unoccupied orbitals of **S**, taken together, spans $T_1 + T_2$ and that these levels will be close to nonbonding. It is therefore plausible that they are partially matched by the two nonbonding E levels in the Clar limit.

The order of T_1 and T_2 can be reasoned in the following way. Let us first assume that, from the Fries limit to the Clar limit, the energy levels are only rising or lowering. One bonding B_2 level and one bonding E level will rise in energy when going from the Fries limit to the Clar limit, since they are unmatched by bonding Clar orbitals (Figure 9b). The B_2 level will rise more quickly than the E level, since the B_2 level is matched by an antibonding Clar orbital and the E level by a nonbonding Clar orbital. Both levels will not meet. At the same time, one other E level will slowly lower in energy, from antibonding in Fries to nonbonding in Clar. This E level will necessarily meet the quickly rising B_2 level, and this will happen at $E > 0$. This indicates that the LUMO will have T_2 symmetry and, by applying eq 11, that the HOMO will have T_1 symmetry.

It is also possible to treat the nonleapfrog cages with O_h symmetry. The neighboring squares are always in a zigzag relation (if in the armchair relation the cage is always a leapfrog). Define u as the number of hexagons between two neighboring squares plus one. Then, $u = 3q$ (where q is an integer) corresponds to leapfrog cages and so is already treated in the previous section. For the other cases, one has

$$\Gamma(\mathbf{F_S}, E < 0) - \Gamma(\mathbf{C_S}, E < 0) = B_{2u} - A_{2g} + E_g, \quad \text{for } u = 3q - 1,$$
$$\Gamma(\mathbf{F_S}, E < 0) - \Gamma(\mathbf{C_S}, E < 0) = B_{2g} - A_{2u} + E_u, \quad \text{for } u = 3q + 1,$$
$$\Gamma(\mathbf{C_S}, E = 0) = E_g + E_u \qquad (33)$$

The assumption that the B_2 level, bonding in $\mathbf{F_S}$ and antibonding in $\mathbf{C_S}$, will meet with the E level, antibonding in $\mathbf{F_S}$ and nonbonding in $\mathbf{C_S}$, to form a T_2 level is fully confirmed here, since the other E level (bonding in $\mathbf{F_S}$ and nonbonding in $\mathbf{C_S}$) has the wrong parity. Thus, one can conclude that, for $u = 3q - 1$ ($3q + 1$), the HOMO will have T_{1g} (T_{1u}) symmetry and the LUMO T_{2u} (T_{2g}) symmetry.

Figure 12a shows the correlation diagram for C_8 (O_h, $u = 1$). A B_{2g} level rises from bonding in $\mathbf{F_S}$ to antibonding in $\mathbf{C_S}$. At the same time, an E_g level lowers from antibonding $\mathbf{F_S}$ to nonbonding in $\mathbf{C_S}$. When $\beta_F = \beta_C = \beta$, both levels meet to form an antibonding T_{2g} level. In a similar way, a bonding T_{1u} level is formed. Figure 12b shows the correlation diagram for C_{32} (O_h, $u = 2$). C_{32} is a bit exceptional: six orbitals are both exactly nonbonding at $\beta_F = \beta_C = \beta$, resulting in an open shell. However, they span the predicted symmetry $T_{1g} + T_{2u}$. Apart from this accidental degeneracy in C_{32}, all nonleapfrog (4,6) cages studied in ref 3 fulfill the prediction of a T_1 HOMO and a T_2 LUMO. The size of the HOMO−LUMO gap of the nonleapfrog and leapfrog octahedral (4,6) cages was also compared previously,[3,5] and it was found that the gap of nonleapfrogs was considerably smaller than that of leapfrogs of similar size, in agreement with the results here.

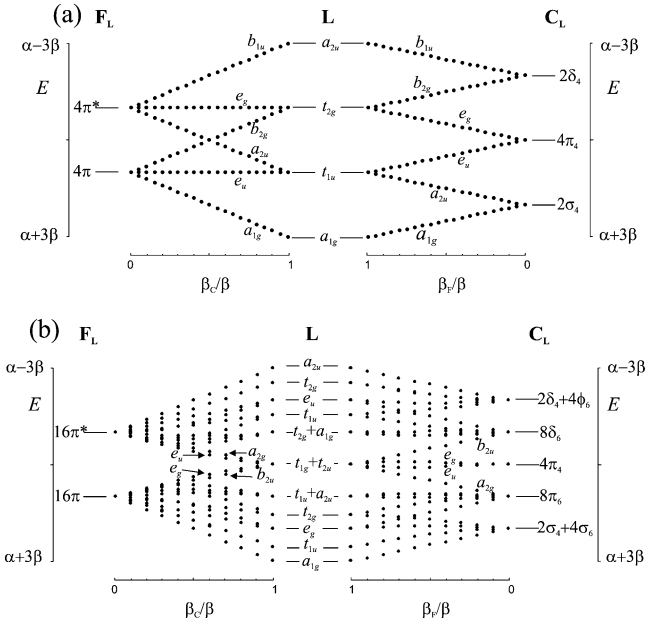

Figure 12. Correlation diagram for octahedral C_8 (a) and C_{32} (b). The conventions are similar to those of Figure 8. The symmetry is reduced from O_h to D_{4h} when β_C or β_F is taken different from β. The D_{4h} symmetry labels are presented for part a, but for part b, only the symmetry labels of the frontier orbitals are shown for clarity reasons. In both cases, a B_2 level is bonding in the Fries limit and antibonding in the Clar limit and vice versa for an A_2 level. At $\beta_F = \beta_C = \beta$, they each combine with an E level, that is nonbonding in the Clar limit, to form T_2 and T_1 levels.

The discussion above only considered the correlation between one Fries/Clar couple. However, there is no single dominant Fries structure, as was the case for leapfrog (4,6) cages. The full two-dimensional correlation diagram can be discussed using the results obtained above. Let us label the three Fries/Clar couples $\mathbf{F}_z/\mathbf{C}_z$, $\mathbf{F}_y/\mathbf{C}_y$, and $\mathbf{F}_x/\mathbf{C}_x$. The two Clar squares in $\mathbf{C}_z$ are placed along the z axis ($\mathbf{C}_x$ and $\mathbf{C}_y$ are similarly defined). At any point in the triangle in Figure 4, the symmetry is at least D_2, with symmetry labels A, B_1, B_2, and B_3. Since in the following discussion symmetry labels of different point groups are used, we also note between square brackets the point group and as a superscript the orientation of the eventual principal axis. Figure 13a shows the correlation diagram along the circumference of the master triangle for the $B_1[D_2]$ representations. This diagram is again nothing more than a superposition of correlations between different Kékulé structures of isolated hexagons and squares. From the discussion based on one Fries/Clar couple, we know that the same $A_2[D_4^z]$ level is antibonding in $\mathbf{F}_z$ and bonding in $\mathbf{C}_z$. From Figure 13a, it is clear that the only way in which this level can end up in the bonding part of $\mathbf{C}_z$ is by following the straight lowering line from $\mathbf{F}_z$ to $\mathbf{F}_y$.

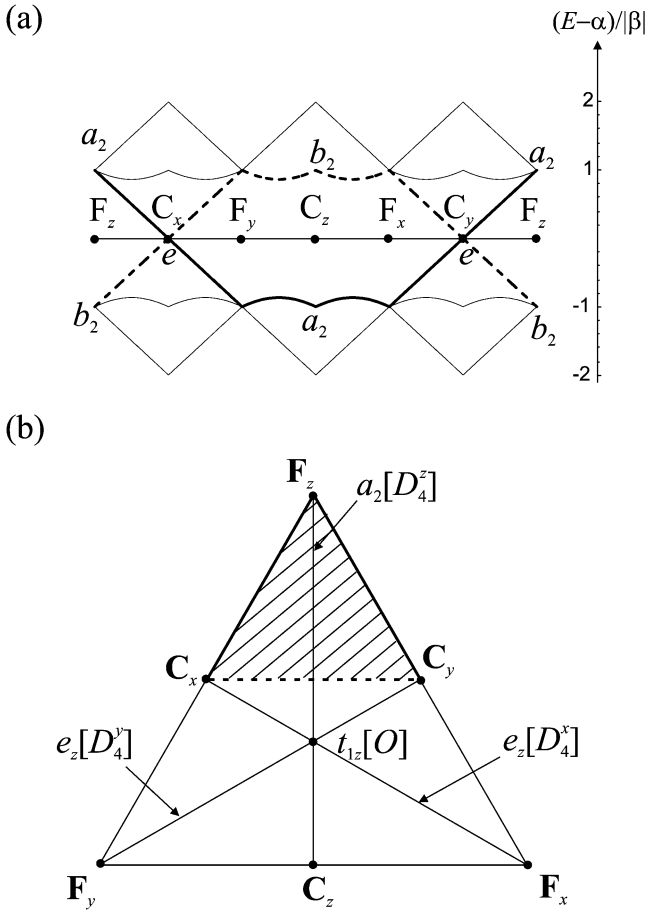

Figure 13. (a) Correlation diagram for the $B_1[D_2]$ representations of an octahedral nonleapfrog (4,6) cage, bigger than the cube, following the circumference of the master triangle in Figure 4. At any of the black dots, the symmetry is D_4, with the principal axis given by the subscript of $\mathbf{F}_i$, $\mathbf{C}_i$. Between these points, the symmetry is D_2. The thick line corresponds to the $B_1[D_2]$ level that has $A_2[D_4^z]$ symmetry at $\mathbf{F}_z$ and $\mathbf{C}_z$, and the thick dashed line corresponds to the $B_1[D_2]$ level that has $B_2[D_4^z]$ symmetry at $\mathbf{F}_z$ and $\mathbf{C}_z$. (b) The two-dimensional correlation diagram for the $B_1[D_2]$ level following the thick line in part a. At any general point in the triangle, the symmetry is D_2. The level is antibonding in the upper part (hatched) of the master triangle and bonding in the lower part. The exact nonbonding frontier is simplified here by the dashed line [$\mathbf{C}_x$, $\mathbf{C}_y$]. The center of the triangle, where the level has $T_{1z}[O]$ symmetry, is a bit below this line, suggesting it will be weakly bonding. Similar arguments apply for the $B_1[D_2]$ level following the dashed line in part a.

In the middle between $\mathbf{F}_z$ and $\mathbf{F}_y$, $\mathbf{C}_x$, the level converts from antibonding to bonding and is part of a $E[D_4^x]$ representation. From $\mathbf{F}_y$ to $\mathbf{C}_z$, the level stays bonding. Exactly the same picture is obtained when following the path [$\mathbf{F}_z$, $\mathbf{C}_y$, $\mathbf{F}_x$, $\mathbf{C}_z$]. For the $B_2[D_4^z]$ level, bonding in $\mathbf{F}_z$ and antibonding in $\mathbf{C}_z$, similar arguments apply. For the cube, only the straight lines in Figure 13a are present, but the general conclusions remain the same.

It is now clear that the same $B_1[D_2]$ level will be bonding in the lower part of the master triangle and antibonding in the upper part (Figure 13b). The shape of the nonbonding frontier line is not known, but it will be close to the line [$\mathbf{C}_x$, $\mathbf{C}_y$]. At the center of the triangle, the level becomes part of a $T_1[O]$ representation. Since this center lies a bit below the line [$\mathbf{C}_x$, $\mathbf{C}_y$], the level is probably slightly bonding. Equation 11 then dictates a slightly antibonding $T_2[O]$ level. Hence, the use of the full two-dimensional correlation diagram only confirms the conclusions from the previous discussion, where only the line [$\mathbf{F}_z$, $\mathbf{C}_z$] was followed.

8. Conclusions and Discussion

Using a group-theoretical analysis, we have predicted the symmetry and number of low-lying orbitals for three different polyhedral cages. The leapfrog (3,6) cages have two nonbonding occupied orbitals with the symmetry Γ_2 below the first empty orbital, and hence, they can act as electron donors. The leapfrog (4,6) cages have a rather large HOMO−LUMO gap, and the symmetry of the highest six occupied orbitals is spanned by $\Gamma_{-1} \times (\Gamma_T + \Gamma_R)$, while the symmetry of the lowest six unoccupied orbitals is spanned by $\Gamma_T + \Gamma_R$. The octahedral nonleapfrog (4,6) cages have a small HOMO−LUMO gap, and the symmetry of the HOMO (LUMO) is given by T_1 (T_2).

We have not applied the analysis for nonleapfrog (4,6) cages with a symmetry lower than *O*. It is however obvious that, when the symmetry is too low, the crossing of energy levels from bonding to antibonding and vice versa between the Fries and Clar limits cannot occur.

Alternating boron nitride (4,6) cages are more chemically plausible and probably already synthesized,[13,14] as opposed to their carbon counterparts. A simple relationship exists between the Hückel MOs of the carbon cage and its boron nitride version and their symmetries,[4,3] so the results given here are also relevant for this type of cages.

Acknowledgment. Financial support from the Belgian Government through the Concerted Action Scheme (GOA) and from the KULeuven Research Council (BOF) is gratefully acknowledged. The authors are indebted to Patrick Fowler (Exeter) for fruitful discussions on the topic.

References and Notes

(1) Fowler, P. W.; Ceulemans, A. *J. Phys. Chem.* **1995**, *99*, 508.

(2) Ceulemans, A.; Compernolle, S.; Delabie, A.; Somers, K.; Chibotaru, L. F.; Fowler, P. W.; Marganska, M. J.; Szopa, M. J. *Phys. Rev. B* **2002**, *65*, 115412.

(3) Compernolle, S.; Ceulemans, A. *Phys. Rev. B*, submitted for publication.

(4) Zhu, H. Y.; Klein, D. J.; Seitz, W. A.; March, N. H. *Inorg. Chem.* **1995**, *34*, 1377.

(5) Zhu, H. Y.; Schmalz, T. G.; Klein, D. J. *Int. J. Quantum Chem.* **1997**, *63*, 393.

(6) Sun, M. L.; Slanina, Z.; Lee, S. L. *Chem. Phys. Lett.* **1995**, *233*, 279.

(7) Slanina, Z.; Sun, M. L.; Lee, S. L. *Nanostruct. Mater.* **1997**, *8*, 623.

(8) Silaghi-Dumitrescu, I.; Lara-Ochoa, F.; Bishof, P.; Haiduc, I. *THEOCHEM* **1996**, *367*, 47.

(9) Alexandre, S. S.; Chacham, H.; Nunes, R. W. *Phys. Rev. B* **2001**, *63*, 045402.

(10) Seifert, G.; Fowler, P. W.; Mitchell, D.; Porezag, D.; Frauenheim, T. *Chem. Phys. Lett.* **1997**, *268*, 352.

(11) Rogers, K. M.; Fowler, P. W.; Seifert, G. *Chem. Phys. Lett.* **2000**, *332*, 43.

(12) Fowler, P. W.; Heine, T.; Mitchell, D.; Schmidt, R.; Seifert, G. *J. Chem. Soc., Faraday Trans.* **1996**, *92*, 2197.

(13) Stephan, O.; Bando, Y.; Loiseau, A.; Willaime, F.; Shramchenko, N.; Tamiya, T.; Sato, T. *Appl. Phys. A* **1998**, *67*, 107.

(14) Golberg, D.; Bando, Y.; Stephan, O.; Kurashima, K. *Appl. Phys. Lett.* **1998**, *73*, 2441.

(15) Fowler, P. W.; Cremona, J. E.; Steer, J. I. *Theor. Chim. Acta* **1988**, *73*, 1.

(16) Deza, M.; Dutour, M. http://www.arxiv.org/abs/math.GT/0212352, 2003.

(17) Fowler, P. W.; Steer, J. I. *J. Chem. Soc., Chem. Commun.* **1997**, *18*, 1403.

(18) Fowler, P. W.; Pisanski, T. *J. Chem. Soc., Faraday Trans.* **1994**, *90*, 2865.

(19) Ceulemans, A.; Fowler, P. W. *Nature* **1991**, *353*, 52.

(20) Cvetković, D. M.; Doob, M.; Sachs, H. *Spectra of graphs: theory and application*; Academic Press: New York, 1979.

(21) Dewar, M. J. S. *The Molecular Orbital Theory of organic chemistry*; McGraw-Hill: New York, 1969.
(22) Halevi, E. A. *Orbital Symmetry and Reaction Mechanism, The OCAMS view*; Springer-Verlag: New York, 1992.
(23) Manolopoulos, D. E.; Woodall, D. R.; Fowler, P. W. *J. Chem. Soc., Faraday Trans.* **1992**, *88*, 2427.
(24) Fowler, P. W.; Rogers, K. M. *J. Chem. Soc., Faraday Trans.* **1998**, *94*, 2509.